Cell Reports, Volume *34*

Supplemental Information

Functional Genomics Identify Distinct and Overlapping Genes Mediating Resistance to Different Classes of Heterobifunctional Degraders of Oncoproteins

Ryosuke Shirasaki, Geoffrey M. Matthews, Sara Gandolfi, Ricardo de Matos Simoes, Dennis L. Buckley, Joseline Raja Vora, Quinlan L. Sievers, Johanna B. Brüggenthies, Olga Dashevsky, Haley Poarch, Huihui Tang, Megan A. Bariteau, Michal Sheffer, Yiguo Hu, Sondra L. Downey-Kopyscinski, Paul J. Hengeveld, Brian J. Glassner, Eugen Dhimolea, Christopher J. Ott, Tinghu Zhang, Nicholas P. Kwiatkowski, Jacob P. Laubach, Robert L. Schlossman, Paul G. Richardson, Aedin C. Culhane, Richard W.J. Groen, Eric S. Fischer, Francisca Vazquez, Aviad Tsherniak, William C. Hahn, Joan Levy, Daniel Auclair, Jonathan D. Licht, Jonathan J. Keats, Lawrence H. Boise, Benjamin L. Ebert, James E. Bradner, Nathanael S. Gray, and Constantine S. Mitsiades

SUPPLEMENTAL INFORMATION

Supplemental Figure legends

Figure S1: *In vitro* activity of CRBN-based degraders against human MM cell lines [Related to Figure 1]

(A-B) *In vitro* activity of dBET6, dBET1 or JQ1 against human MM cell lines.

(**A**) CTG assays were performed to quantify the viability of human MM cell lines treated for 72h with increasing concentrations of the BET bromodomain degronimids dBET1 and dBET6. Based on these results, dBET6 was selected for the remainder of this study as a representative of this class of compounds (results represent averages +/- SE from three independent replicates for each experimental condition). (**B**) Comparison of the effects of dBET6 vs. JQ1 treatment (48h) on the human MM cell lines MM.1S, RPMI-8226 or JJN3 (CS-BLI assay).

(C-H) Immunoblotting analyses of degronimid-treated MM.1S cells. MM.1S cells were treated with dBET6, Thal-SNS-032 or JQ1 (0.001, 0.01, 0.1, 1 μM) or DMSO control for 4 h. Immunoblotting analyses were performed to examine the protein levels for (**C**) BRD2; (**D**) BRD3; (**E**) BRD4; (**F**) MYC; and (**G,H**) CDK9. Each panel represents a different blot, incubated with the antibody for the corresponding target protein and (for panels **C-G**) GAPDH as a loading control within the same blot. Panel **H** has been probed with only anti-CDK9 antibody, to highlight more clearly the 2 known CDK9 isoforms, an abundant 42 kDa isoform and a less abundant isoform of higher molecular weight.

(I-K) Evaluation of anti-MM activity of dBET6 after exposure to different durations of treatment or in co-cultures with bone marrow stromal cells.

(**I-J**) Representative plots (**I**) from flow cytometry assessment (48h) for Annexin-V (AnnV) and propidium iodide (PI) staining of MM.1S cells treated with dBET6 (0.01μM or 0.05μM) or vehicle, followed by washout after 4h, 8h vs. no washout, to examine whether dBET6 induces a dose- and time-dependent increase in Annexin V-positive/PI-negative apoptotic cells and Annexin V-positive/PI-positive necrotic cells. (**J**) Corresponding dose-response curves (48h) of MM.1S cells treated with dBET6 with and without drug-washout. Data are reported as the average +/-SE of four independent experiments.

(**K**) CS-BLI viability assays of luciferase-expressing human MM cell lines cultured alone or with HS-27A bone marrow stromal cells in the presence vs. absence of dBET6 (0, 0.01, 0.05, 0.1, 0.5 and 1 μM, 48h) were performed to quantify the dBET6-induced reduction of the percentage of viable tumor cells in the presence vs. absence of stromal cells.

Figure S2: Molecular profiling changes *in vitro* and anti-tumor activity *in vivo* of dBET6 treatment [Related to Figure 1]

(A-C) Molecular profiling changes induced in MM cells after pharmacological degradation vs. inhibition of BET bromodomain proteins

(**A**) Transcriptional profiling changes induced in MM cells with pharmacological degradation vs. inhibition of BET bromodomain proteins: MM.1S cells were treated with dBET6 (0.1 μM or 0.5 μM) or JQ1 (0.5 μM) for 4h, harvested and then processed for RNA-seq analysis (n = 3 replicates, A through C, per experimental condition). The heat map depicts a hierarchical clustering of changes in transcriptional profiles induced after treatment with dBET6 vs. JQ1.

(**B-C**) Reverse Phase Protein Array (RPPA) analysis of response to dBET6 in human MM cells: MM.1S cells were treated with dBET6 (0.1 μM) or JQ1 (0.5 μM) (vs. untreated controls [UT]) and harvested after 4 h or 18 h, followed by RPPA. The heat map of panel **B** depicts that 4 h and 18 h of dBET6 treatment reduce the expression of key pro-survival proteins, such as Mcl-1, c-Myc, and pS6, while leading to the upregulation at 18 h of the cell cycle inhibitor p21, and cleavage of executioner caspases (e.g. caspase 3). The altered expression of key proteins that appear important for the pro-apoptotic effects of dBET6 are shown individually (panel **C**; n = 3 independent replicates per condition; results depicted as boxplots highlighting the median and min-max range of signal in each experimental condition).

(D-G) Studies of *in vivo* anti-tumor activity of dBET6 in two xenograft models of human MM cell lines. Human MM.1S cells were transplanted into NSG mice either on the right flank (subcutaneous model, panels **D,E**) or via tail vein injection (diffuse model, panels **F,G**). Treatment with dBET6 (30mg/kg

daily for 8 days) was initiated in the subcutaneous model when tumor size reached approximately 100 mm^3. In the diffuse model, dBET6 treatment (20 mg/kg daily for 12 days) began 1 week post-tumor cell injections. In the model of subcutaneous lesions, we observed that dBET6 treatment significantly suppressed the rate of tumor growth increase compared with vehicle control (**D;** p=0.0004, 2-way analysis of variance for comparison between cohorts over time) and led to a significant increase in overall survival of mice (**E**; p=0.002, log-rank test). In the model of diffuse lesions established after intravenous injections of human MM.1S-Luc+ cells, dBET6 treatment led to significantly lower tumor burden, measured by BLI, compared with vehicle control (**F;** p=0.001, 2-way analysis of variance for comparison between cohorts over time), but only minimal overall survival advantage was detected (**G**; p=0.004, log-rank test). Results in panels **D** and **F** represent averages +/- SE.

Figure S3: Human MM cells with prior exposure to and tolerance against other agents can remain sensitive to dBET6 [Related to Figure 1]. Pools of human MM.1S-Cas9+ cells transduced with a lentiviral genome-scale library (GeCKO v2) of sgRNAs were treated with JQ1 (500 nM) or bortezomib (25 nM), with at least 3 rounds of treatment per compound. These drug-exposed populations of MM cells were then tested in dose-response CTG assays (**A-B**), to document tolerance of these surviving cells to the respective agents. (**C**) Cells with prior exposure to and tolerance to JQ1 or bortezomib do not exhibit resistance to dBET6. (**D**) Bone marrow aspirates obtained from individuals with MM (with different disease status and patterns of prior exposure to and resistance/refractoriness to currently available clinical treatments) and one individual with MGUS were processed for selection of CD138+ plasma cells. CD138+ cells were then treated with dBET6 or vehicle control. Cell viability was assessed using CTG and individual patient results (average +/- SE) are shown (RR = relapsed/refractory disease; ND = newly diagnosed disease; MGUS = monoclonal gammopathy of undetermined significance) (Panels **A-C** depict averages +/- SE of 3 distinct experiments for each panel; panels **A-D** included triplicates for each condition in each distinct experiment).

Figure S4: Schematic overview of genome-scale CRISPR-based functional genomics studies to characterize the mechanisms of tumor cell resistance to CRBN- or VHL-mediated pharmacological "degraders" of oncoproteins [Related to Figures 1, 2, 3 and 4].
We performed genome-scale CRISPR/Cas9 gene editing screens (detailed information included in STAR Methods). Briefly, MM.1S-Cas9+ cells were transduced with pooled lentiviral particles containing genome-scale sgRNA libraries (GeCKOv2 or *Brunello*; as indicated in each experiment) and then studied in 3 distinct types of screens, which involved: i) "short-term" (48 h) treatments with either dBET6 or Thal-SNS-032, followed by tumor cell collection at the end of the treatment; ii) "long-term" studies with successive rounds of dBET6, Thal-SNS-032, ARV-771 or MZ-1 treatment of the pools of MM.1S cells with genome-scale CRISPR-based gene editing, allowing re-growth between treatments and until *in vitro* drug sensitivity testing confirmed the selection of pools of MM.1S cells with significant shift-to-the-right of their dose-response curve (compared to degrader-naive controls) for the respective treatment; and iii) "extended degronimid treatment" screens, in which Thal-SNS-032-resistant MM.1S *Cas9*+ cell populations isolated from our initial "long-term" CRISPR/Cas9-based gene editing screen continue receiving additional degronimid treatment for 2 weeks, with either Thal-SNS-032 (i.e., a continuation of the treatment which had led to the isolation of these treatment-resistant cells) or dBET6.

Figure S5: Functional studies to validate the role of individual candidate resistance genes derived from genome-scale CRISPR-based gene editing studies [Related to Figures 1, 2 and 3].
(**A**) MM.1S-Cas9+ cells transduced with sgRNAs against *VHL, CRBN* or (serving as controls) sgRNAs against the olfactory receptor genes *OR2S2, OR12D2 and OR5AU1* were tested for their *in vitro* response to ARV-771 (left panel) or dBET6 (right panel) (CTG assays, 72 h).
(**B**) KMS-11-Cas9+ cells transduced with sgRNAs against *VHL* or (serving as controls) sgRNAs against the olfactory receptor genes *OR2H1, OR12D2, OR5V1, OR5AU1 and OR10G2* were tested for their *in vitro* response to ARV-771 (left panel) or dBET6 (right panel) (CTG assays, 72 h).
(**C**) MM.1S-Cas9+ cells transduced with sgRNAs against *TCEB1, TCEB2, CUL2, FBXW2, UBE2R2* or (serving as controls) sgRNAs against the olfactory receptor genes *OR2H1* and *OR12D2* were tested for their *in vitro* response to ARV-771 (left panel) or dBET6 (right panel) (CTG assays, 72 h).

(**D**) Results of insertion/deletion (INDEL) analyses (using the *CRISPResso2* algorithm) from "competition" assays in which MM.1S-Cas9+ cells transduced with sgRNAs against *UBE2R2* or the olfactory receptor (OR) gene *OR2S2* were mixed in 1:9 ratio and then cultured in the presence of ARV-771 or DMSO control. The x-axis represents the position (relative to the 3' of the primer for the sequencing analysis) of each nucleotide of the amplicon containing the *UBE2R2* sgRNA cut-site, while the y-axis depicts the fraction of reads with INDELs in each respective position of the amplicon. The ARV-771-treated pool of cells with sg*UBE2R2* and sg*OR* (red curve) exhibits higher fraction of INDELs in the *UBE2R2* amplicon compared to the control DMSO-treated pool of cells with sg*UBE2R2* and sg*OR* (orange curve); the latter pool had very similar distribution of INDELs as the baseline (pre-treatment) mixture of cells with sg*UBE2R2* and sg*OR* (black line). The grey curve depicts, as a control, the results for the population of cells with only sg*OR.*
(Panels **A-C** depict averages +/- SE triplicates for each condition)

Figure S6: (A-B) CRISPR-based gene activation studies using genome-scale sgRNA libraries [Related to Figures 1, 2 and 3].
We performed whole-genome CRISPR/Cas9-based gene activation screens to evaluate in a pooled manner which genes may be implicated through their gain-of-function in the development of resistance by MM.1S cells against (**A**) dBET6 or (**B**) ARV-771. For each panel, results depict the average $\log_2$ fold-change (of 3 experimental replicates per condition) of normalized read counts of sgRNAs for each gene in dBET6- or ARV-771-treated MM.1S cells vs. the respective vehicle control MM.1S cells. *ABCB1* was the only gene with sgRNA enrichment (3-4 of 4 sgRNAs per gene, $p<0.05$ [rank aggregation algorithm], $\log_2FC>1.0$) in either screen.
(C-D) LOF events typically associated with "high-risk" / biologically aggressive MM are not enriched among cells resistant to either CRBN- or VHL-based degraders. Overview of results for key examples of genes whose LOF events are recurrently observed in MM and/or associated with adverse clinical outcomes. Depicted results refer to the "long-term" genome-scale CRISPR-based gene editing LOF screens for resistance to degraders operating through either (**C**) CRBN (dBET6 and Thal-SNS-032) or (**D**) VHL (ARV-771 and MZ-1).

Figure S7: Patterns of essentiality for tumor cells *in vitro* in drug-free conditions for genes associated with resistance to CRBN- or VHL-mediated pharmacological degraders of oncoproteins [Related to Figure 5].
Color-coded heatmaps depict CERES scores, as a quantitative metric of relative dependence of human tumor cell lines, based on CRISPR-based gene editing screens (*AVANA* sgRNA library) performed *in vitro* in the absence of drug treatment. CERES scores for MM cell lines (plus the HUNS1 cell line which is reported to be a MM line but also has lymphoblast features) are depicted as a matrix (right side of the graph) of cell lines (in columns) and genes (in rows); whereas for non-MM lines data are depicted for each gene (row) in stacked bar graphs, to visualize the CERES scores in descending order (from left to right) for each gene. The figure depicts results for genes associated with resistance to degronimids (blue gene symbols), VHL-mediated degraders (red gene symbols) or both (black gene symbols), as these genes emerged as top "hits" from "long-term" (i.e., until identification of pools of cells with significant shift-to-the-right for their dose-response curve) CRISPR screens for "degrader" resistance. As indicated in the color-coded scale, black or dark blue color indicates that a gene has CERES scores compatible with pronounced sgRNA depletion in a given cell line.

Figure S8: Patterns of co-occurrence of essentiality and high transcript levels for known or presumed E3 ligase genes in tumor cell lines [Related to Figure 5].
(**A-C**) Known or presumed E3 ligase genes are examined, based on data from the Dependency Map CRISPR-based gene editing screens (*AVANA* sgRNA library; screens performed *in vitro* in the absence of drug treatment), for the percentage of "high-expressor" cell lines (i.e. cell lines with transcript levels for a given E3 ligase above the average + 2SD of a broad range of normal tissues in the GTEx database, similarly to the analyses in Figure 5B) and the % of "high-expressor" cell lines with CERES scores <-0.5 for that same E3 ligase. Results are depicted for (**A**) all cell lines of the Dependency Map CRISPR-based gene editing screens, irrespective of p53 mutational status; (**B**) p53 (*TP53*)-mutant cell lines; and (**C**) p53

wild-type cell lines. Gene symbols in the red or blue boxes represent known E3 ligases (bold black), members of complexes with E3 ligase activity (black) or presumed E3 ligases (grey) with ≥25% "high-expressor" cell lines & CERES scores <-0.5 in at least 2/3 of "high-expressor" cell lines among p53-mutant cell lines (red box in panel **B**) or all cell lines irrespective of p53 mutational status (blue box, in panel **A**).
(**D**) Distribution of CERES scores for essentiality of *MDM2* in p53-mutant vs. p53 wild-type cell lines ($p<0.0001$, t-test).
(**E**) Distribution of CERES scores in MM vs. non-MM cell lines for key genes highlighted in panels (**A**-**C**).

Supplemental Figure S1

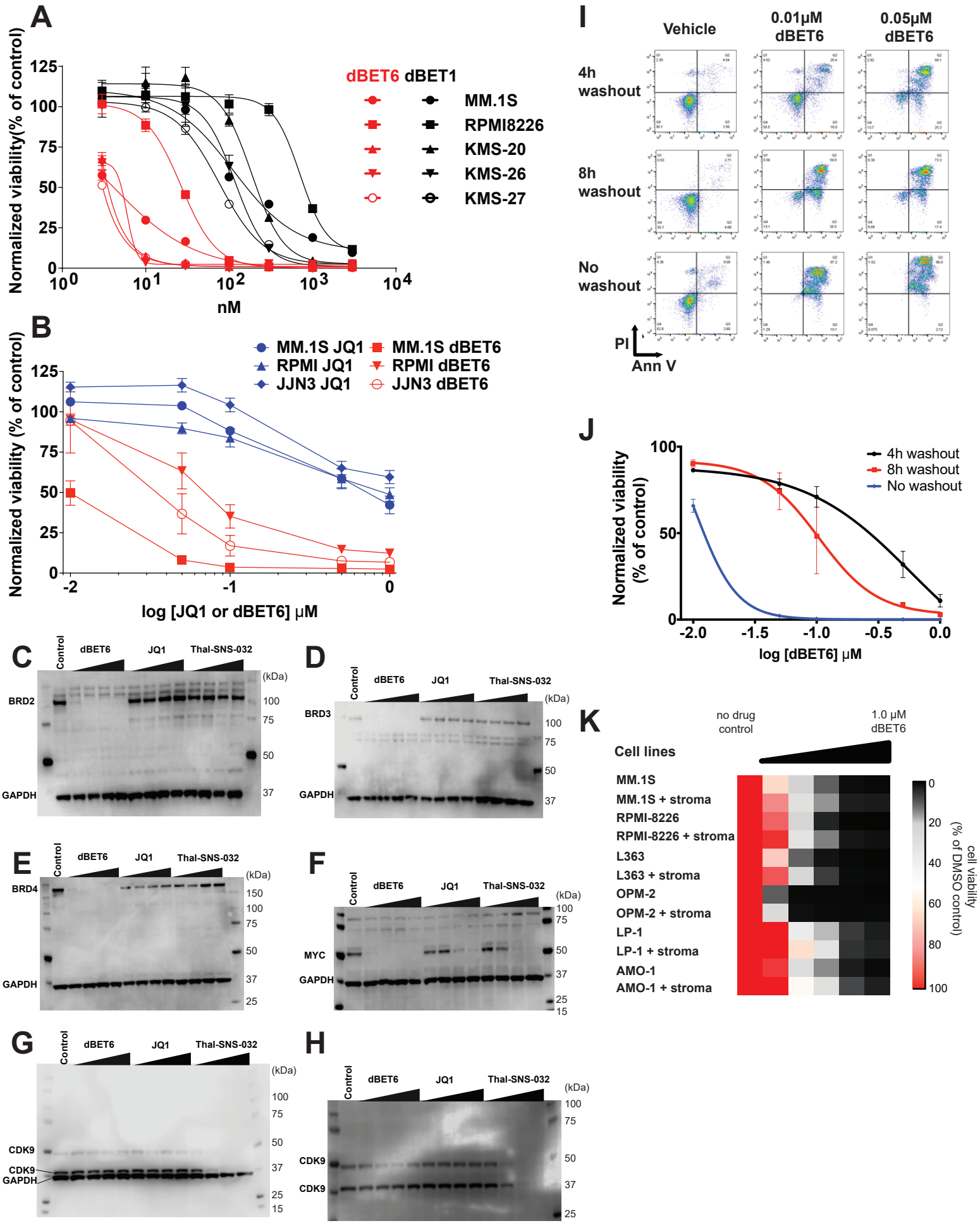

Supplemental Figure S2

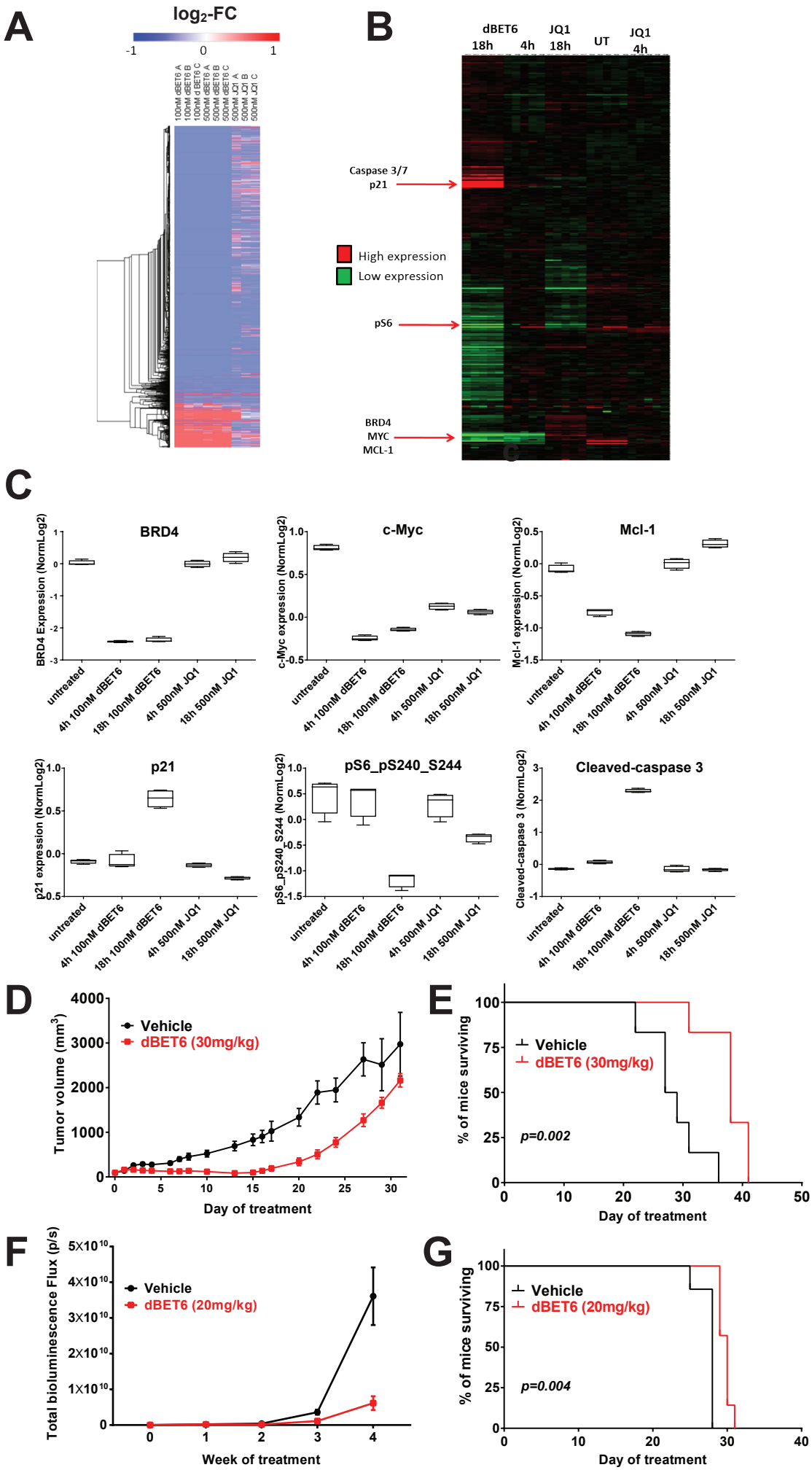

Supplemental Figure S3

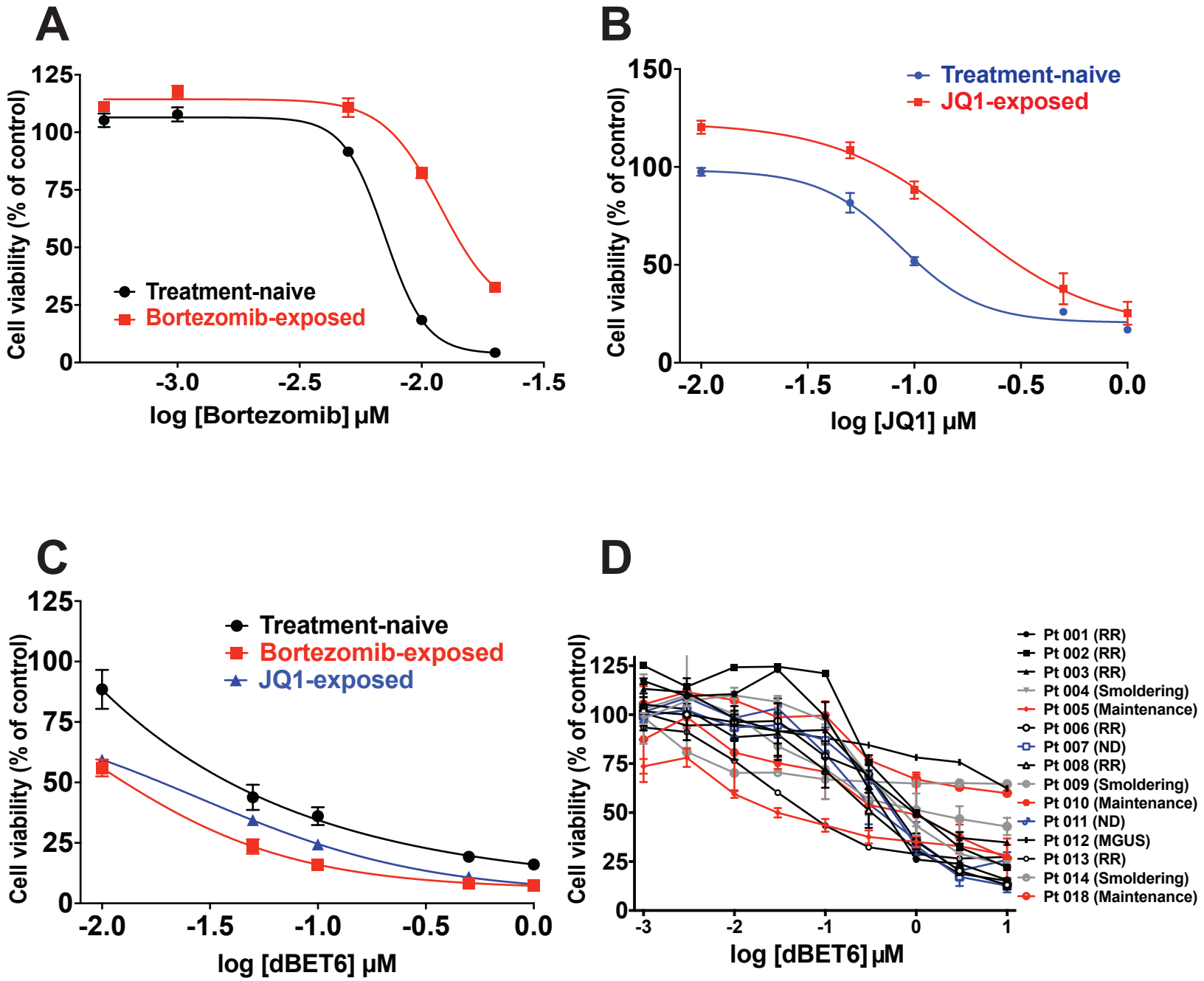

Supplemental Figure S4

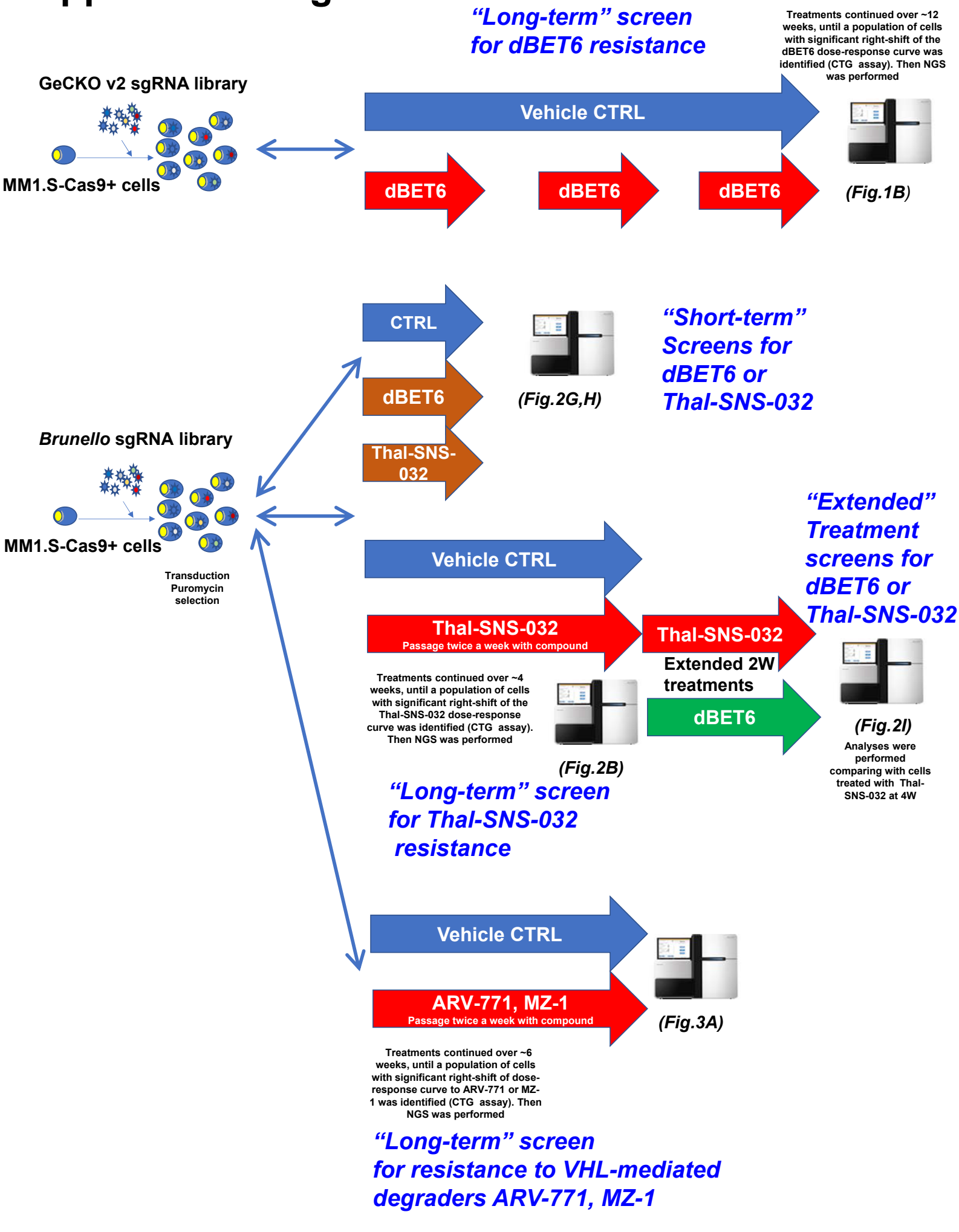

Supplemental Figure S5

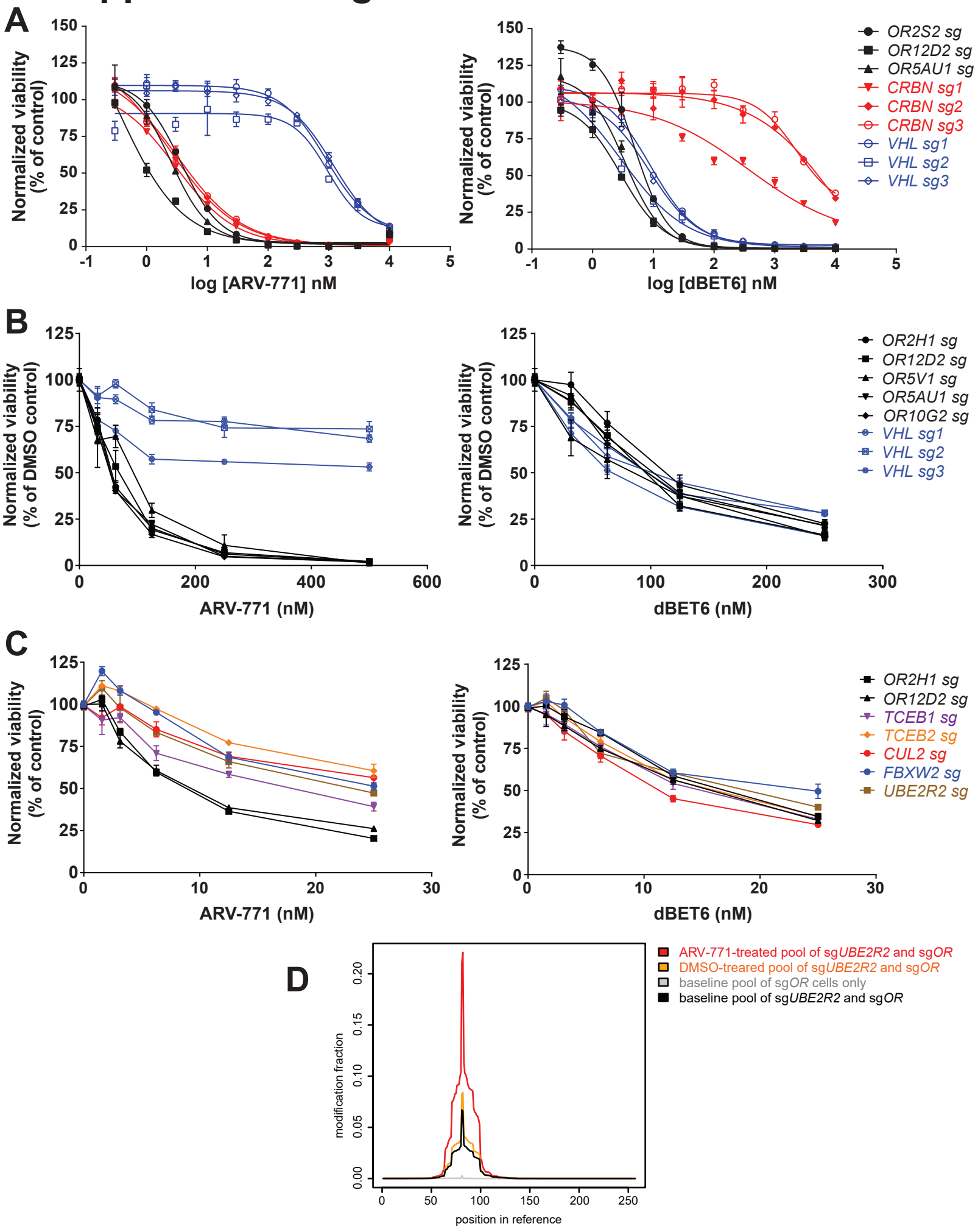

Supplemental Figure S6

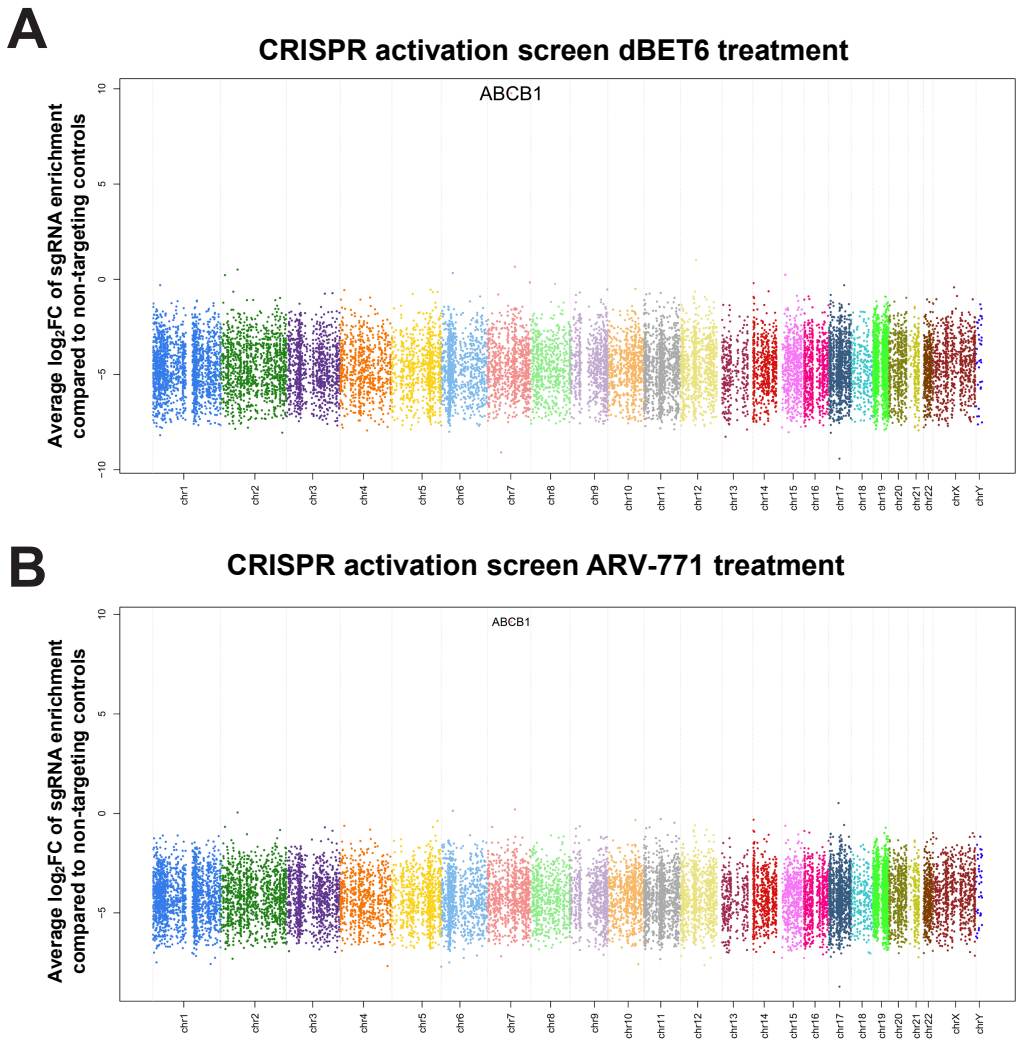

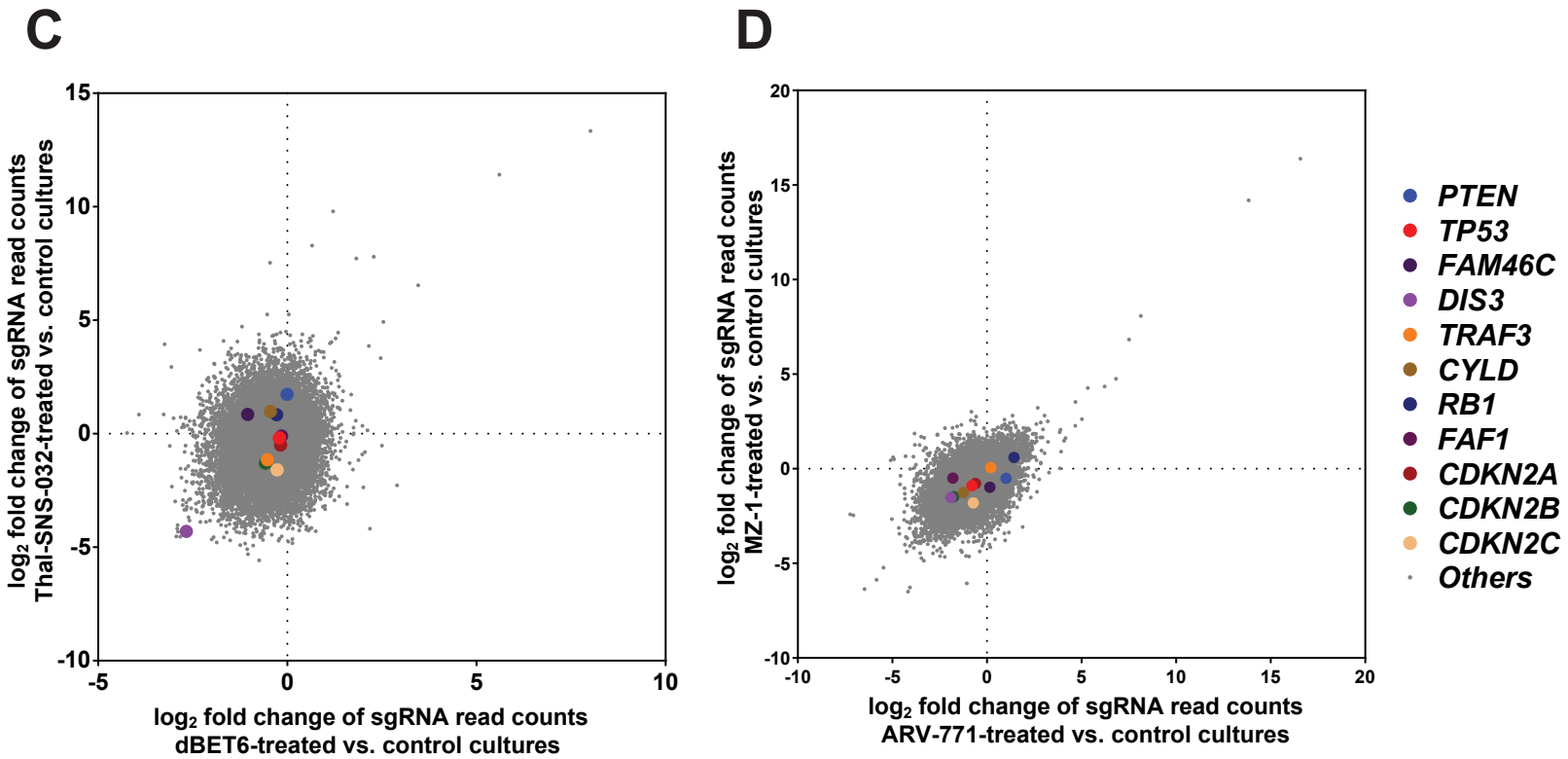

Supplemental Figure S7

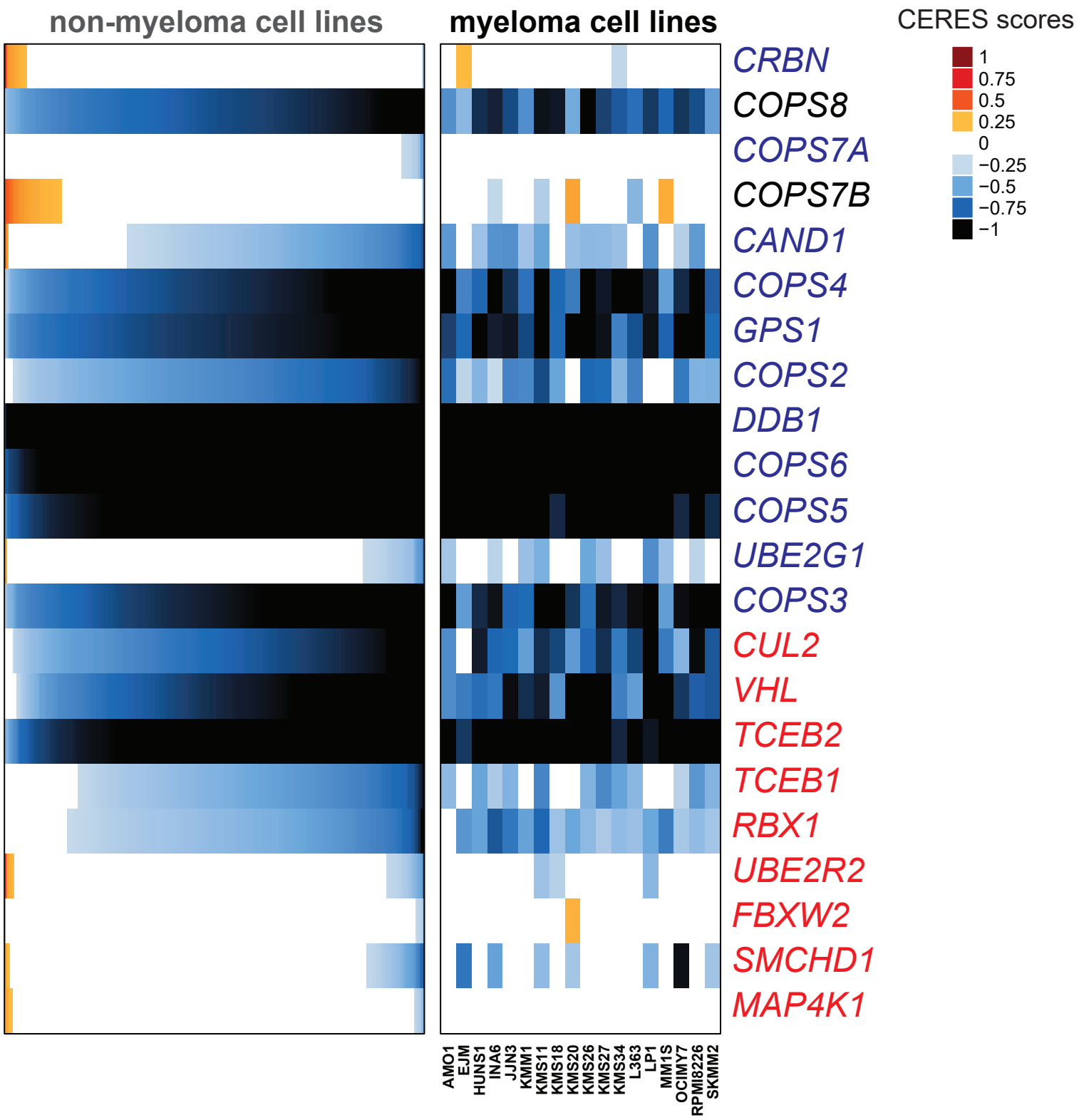

Supplemental Figure S8

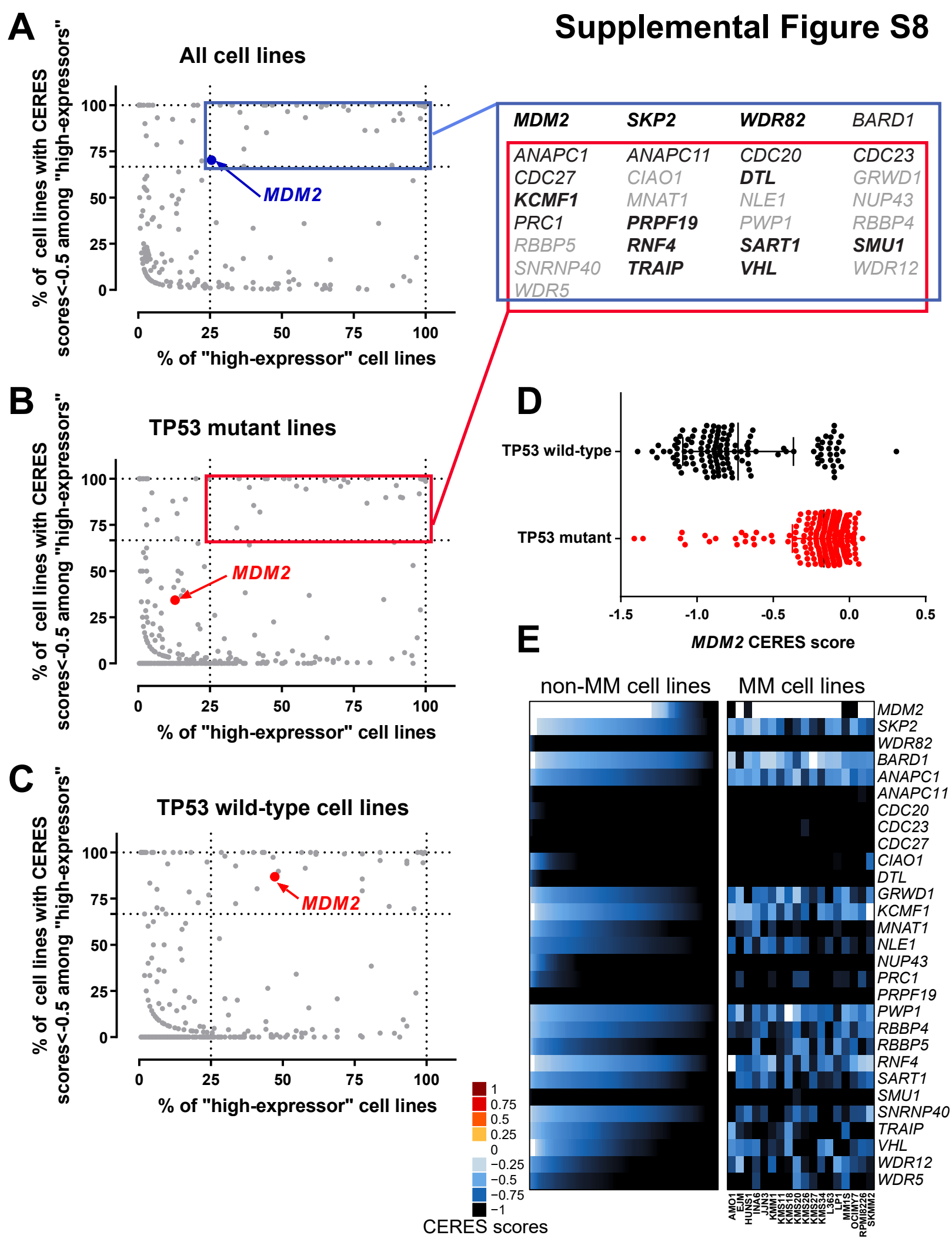

Table S1: List of primers

Primers:						
		TM°c	Size	GC %	Barcode	Rev. comp. barcode
F1	AATGGACTATCATATGCTTACCGTAACTTGAAAGTATTTCG	69.2	41	34.1		
R1	CTTTAGTTTGTATGTCTGTTGCTATTATGTCTACTATTCTTTCC	68.3	44	31.8		
R21	CAAGCAGAAGACGGCATACGAGATCCTCTCTGGTGACTGGAGTTCAG ACGTGTGCTCTTCCGATCTtctactattctttcccctgcact	79.2	89	50.6	CCTCT CTG	CAGAG AGG
R22	CAAGCAGAAGACGGCATACGAGATCTAGTACG GTGACTGGAGTTCAG ACGTGTGCTCTTCCGATCTtctactattctttcccctgcact	79.2	89	50.6	CTAGT ACG	CGTAC TAG
R23	CAAGCAGAAGACGGCATACGAGATTTCTGCCT GTGACTGGAGTTCAG ACGTGTGCTCTTCCGATCTtctactattctttcccctgcact	79.2	89	50.6	TTCTG CCT	AGGCA GAA
R24	CAAGCAGAAGACGGCATACGAGATGCTCAGGA GTGACTGGAGTTCAG ACGTGTGCTCTTCCGATCTtctactattctttcccctgcact	79.2	89	50.6	GCTCA GGA	TCCTG AGC
R25	CAAGCAGAAGACGGCATACGAGATAGGAGTCC GTGACTGGAGTTCAG ACGTGTGCTCTTCCGATCTtctactattctttcccctgcact	79.2	89	50.6	AGGAG TCC	GGACT CCT
R26	CAAGCAGAAGACGGCATACGAGATCATGCCTA GTGACTGGAGTTCAG ACGTGTGCTCTTCCGATCTtctactattctttcccctgcact	79.2	89	50.6	CATGC CTA	TAGGC ATG
R27	CAAGCAGAAGACGGCATACGAGATGTAGAGAG GTGACTGGAGTTCAG ACGTGTGCTCTTCCGATCTtctactattctttcccctgcact	79.2	89	50.6	GTAGA GAG	CTCTCT AC
R28	CAAGCAGAAGACGGCATACGAGATAACAATGGGTGACTGGAGTTCAG ACGTGTGCTCTTCCGATCTtctactattctttcccctgcact	79.2	89	50.6	AACAA TGG	CCATT GTT
R29	CAAGCAGAAGACGGCATACGAGATAGCGTAGCGTGACTGGAGTTCAG ACGTGTGCTCTTCCGATCTtctactattctttcccctgcact	79.2	89	50.6	AGCGT AGC	GCTAC GCT
R210	CAAGCAGAAGACGGCATACGAGATCAGCCTCGGTGACTGGAGTTCAG ACGTGTGCTCTTCCGATCTtctactattctttcccctgcact	79.2	89	50.6	CAGCC TCG	CGAGG CTG
R211	CAAGCAGAAGACGGCATACGAGATAGTAGCGTGTGACTGGAGTTCAG ACGTGTGCTCTTCCGATCTtctactattctttcccctgcact	79.2	89	50.6	AGTAG CGT	ACGCT ACT
R212	CAAGCAGAAGACGGCATACGAGATCAGTGAGTGTGACTGGAGTTCAG ACGTGTGCTCTTCCGATCTtctactattctttcccctgcact	79.2	89	50.6	CAGTG AGT	ACTCA CTG
R213	CAAGCAGAAGACGGCATACGAGATCGTACTCAGTGACTGGAGTTCAG ACGTGTGCTCTTCCGATCTtctactattctttcccctgcact	79.2	89	50.6	CGTAC TCA	TGAGT ACG
R214	CAAGCAGAAGACGGCATACGAGATCTACGCAGGTGACTGGAGTTCAG ACGTGTGCTCTTCCGATCTtctactattctttcccctgcact	79.2	89	50.6	CTACG CAG	CTGCG TAG
R215	CAAGCAGAAGACGGCATACGAGATGGAGACTAGTGACTGGAGTTCAG ACGTGTGCTCTTCCGATCTtctactattctttcccctgcact	79.2	89	50.6	GGAGA CTA	TAGTCT CC
R216	CAAGCAGAAGACGGCATACGAGATAGGTAAGGGTGACTGGAGTTCAG ACGTGTGCTCTTCCGATCTtctactattctttcccctgcact	79.2	89	50.6	AGGTA AGG	CCTTA CCT
R217	CAAGCAGAAGACGGCATACGAGATAACGCATTGTGACTGGAGTTCAGA CGTGTGCTCTTCCGATCTtctactattctttcccctgcact	79.2	89	50.6	AACGC ATT	AATGC GTT
R218	CAAGCAGAAGACGGCATACGAGATACAGGTATGTGACTGGAGTTCAG ACGTGTGCTCTTCCGATCTtctactattctttcccctgcact	79.2	89	50.6	ACAGG TAT	ATACCT GT

F2	AATGATACGGCGACCACCGAGATCTACACTCTTTCCCTACACGACGCT CTTCCGATCT**tc**ttgtggaaaggacgaaacaccg	79.4	82	51.2		
F2S1	AATGATACGGCGACCACCGAGATCTACACTCTTTCCCTACACGACGCT CTTCCGATCTA**tc**ttgtggaaaggacgaaacaccg	79.1	83	50.6		
F2S2	AATGATACGGCGACCACCGAGATCTACACTCTTTCCCTACACGACGCT CTTCCGATCTTA**tc**ttgtggaaaggacgaaacaccg	79.1	84	50		
F2S3	AATGATACGGCGACCACCGAGATCTACACTCTTTCCCTACACGACGCT CTTCCGATCTGTA**tc**ttgtggaaaggacgaaacaccg	79.2	85	50.6		
F2S4	AATGATACGGCGACCACCGAGATCTACACTCTTTCCCTACACGACGCT CTTCCGATCTCGTA**tc**ttgtggaaaggacgaaacaccg	79.2	86	51.2		
F2S5	AATGATACGGCGACCACCGAGATCTACACTCTTTCCCTACACGACGCT CTTCCGATCTACGTA**tc**ttgtggaaaggacgaaacaccg	79.2	87	50.6		
F2S6	AATGATACGGCGACCACCGAGATCTACACTCTTTCCCTACACGACGCT CTTCCGATCTGACGTA**tc**ttgtggaaaggacgaaacaccg	79.3	88	51.1		
F2S7	AATGATACGGCGACCACCGAGATCTACACTCTTTCCCTACACGACGCT CTTCCGATCTAGACGTA**tc**ttgtggaaaggacgaaacaccg	79.1	89	50.6		
F2S8	AATGATACGGCGACCACCGAGATCTACACTCTTTCCCTACACGACGCT CTTCCGATCTCAGACGTA**tc**ttgtggaaaggacgaaacaccg	79.3	90	51.1		
F2S9	AATGATACGGCGACCACCGAGATCTACACTCTTTCCCTACACGACGCT CTTCCGATCTTCAGACGTA**tc**ttgtggaaaggacgaaacaccg	79.3	91	50.5		
F2S10	AATGATACGGCGACCACCGAGATCTACACTCTTTCCCTACACGACGCT CTTCCGATCTGTCAGACGTA**tc**ttgtggaaaggacgaaacaccg	79.3	92	51.1		
UBE2R2 Foward	TGCATTTCGATTCTTCATCC	50.8	20	40		
UBE2R2 Reverse	GCTCTTCAAAATGACGCATACA	53.7	20	40.9		

Table S2: List of sgRNAs

Sequence Name	Target Sequence
COPS7B-1	TGGCCGTGACATCCGAAAGA
COPS7B-2	TCTTGATGCCAAGCTCACGA
COPS7B-3	TCTTTCAGCAACACGGAGTA
COPS7B-4	GCATCTTACCATCGTGAGCT
COPS7B-5	TTGTTGAACCTGTTTGCCTA
COPS7B-6	GTGGTTCTCTTTGTACTGGT
COPS2-1	GTGGTGGTAAAATGCACTTG
COPS2-2	TAGTAACTCCGAGCCAAATG
COPS2-3	CCAGTTACATCAGTCGTGCC
COPS2-4	GTGGTTTAAGACAAACACAA
DDB1-1	CATTGTCGATATGTGCGTGG
DDB1-2	GGATAGCCATCTGAATTGAG
DDB1-3	CTACCAACCTGCGATCACCA
DDB1-4	TCGTGTCTTGGACTTCAATG
COPS8-1	AGTATACGCTTGAGAGACCA
COPS8-2	AGAAGCTGACCATACACTGG
COPS8-3	CAACCATCAACGCTCACCAG
COPS8-4	GCAGGCAAATTCTGAACTTG
Non-Targeting (NT) Control 1 (A)	ATCAGCCCATTTCTGCGCAC
Non-Targeting (NT) Control 2 (B)	AGGGGCAGGGCTATCTTATG
Non-Targeting (NT) Control 3 (C)	GCACATCGTTATATACCAGA
Non-Targeting (NT) Control 4 (D)	CAGGGTTGCGCAGAGGACTC
OR2H1	GATGGCCTTTGACCGATACG
OR12D2	GATGGCATTTGACCTCTCTG
OR2S2	GAGAAGGAGATGGTTTCCTG
OR5AU1	GATGAGATAGCACTCACTGG
OR5V1	GAAACCAGCAGCCCAGCATG
OR10G2	GGAGGCTTCTTAGATTTGGG
TCEB1	AGGTCCTTCACAGCCACCAT
TCEB2	GCTTCACCAGTCAAACAGCA
CUL2	AGATATCTATGCTTTATGTG
FBXW2	CAGCATGTGAGTAAAGTCTG
UBE2R2	GGAATCCTACTCAGAATGTG
CRBN sg1	ACCAATGTTCATATAAATGG
CRBN sg2	CTGACTGTGTTCTTAGCTCA
CRBN sg3	TGAAGAGGTAATGTCTGTCC
VHL sg1	CATACGGGCAGCACGACGCG
VHL sg2	CGCCGCATCCACAGCTACCG
VHL sg3	GAGATGCAGGGACACACGAT